JOC Article

Bisphosphonate Derivatives of Nucleoside Antimetabolites: Hydrolytic Stability and Hydroxyapatite Adsorption of 5′-β,γ-Methylene and 5′-β,γ-(1-Hydroxyethylidene) Triphosphates of 5-Fluorouridine and *ara*-Cytidine

Mikko Ora,[†] Tuomas Lönnberg,[†] Diana Florea-Wang,[†] Shawn Zinnen,[‡] Alexander Karpeisky,[‡] and Harri Lönnberg*,[†]

Department of Chemistry, University of Turku, FIN-20014 Turku, Finland, and MBC Pharma Inc., Aurora, Colorado 80047

harlon@utu.fi

Received February 7, 2008

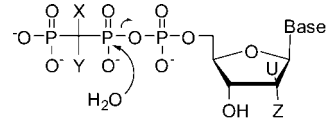

X = Me, Y = OH or X = Y = H
U = H, Z = OH or U = OH, Z = H
Base = Cyt or 5-F-Ura

Kinetics of the hydrolytic reactions of four bisphosphonate derivatives of nucleoside antimetabolites, viz., 5-fluorouridine 5′-β,γ-(1-hydroxyethylidene) triphosphate (**4**), 5-fluorouridine 5′-β,γ-methylene triphosphate (**5**), *ara*-cytidine 5′-β,γ-(1-hydroxyethylidene) triphosphate (**6**), and *ara*-cytidine 5′-β,γ-methylene triphosphate (**7**), have been studied over a wide pH range (pH 1.0−8.5) at 90 °C. With each compound, the disappearance of the starting material was accompanied by formation of the corresponding nucleoside 5′-monophosphate, the reaction being up to 2 orders of magnitude faster with the β,γ-(1-hydroxyethylidene) derivatives (**4**, **6**) than with their β,γ-methylene counterparts (**5**, **7**). With compound **7**, deamination of the cytosine base competed with the phosphate hydrolysis at pH 3−6. The measurements at 37 °C (pH 7.4) in the absence and presence of divalent alkaline earth metal ions (Mg^{2+} and Ca^{2+}) showed no sign of metal ion catalysis. Under these conditions, the initial product, nucleoside 5′-monophosphate, underwent rapid dephosphorylation to the corresponding nucleoside. Hydrolysis of the β,γ-methylene derivatives (**5**, **7**) to the corresponding nucleoside 5′-monophosphates was markedly faster in mouse serum than in aqueous buffer (pH 7.4), the rate-acceleration being 5600- and 3150-fold with **5** and **7**, respectively. In human serum, the accelerations were 800- and 450-fold compared to buffer. In striking contrast, the β,γ-(1-hydroxyethylidene) derivatives did not experience a similar decrease in hydrolytic stability. The stability in human serum was comparable to that in aqueous buffer ($\tau_{1/2}$ = 17 and 33 h with **4** and **6**, respectively), and on going to mouse serum, a 2- to 4-fold acceleration was observed. To elucidate the mineral-binding properties of **4**−**7**, their retention on a hydroxyapatite column was studied and compared to that of zoledronate (**1a**) and nucleoside mono-, di-, and triphosphates.

Introduction

Bisphosphonates, particularly zoledronate (**1a**) or pamidronate (**1b**), are effective bone-specific palliative treatments that reduce tumor-induced skeletal complications.[1] However, there are several limitations on the use of these drugs, which include poor bioavailability (<1−10%), potential for renal toxicity,[2a] and osteonecrosis of the jaw.[2b] In addition to marked bone-seeking and antiresorptive properties, experimental data suggest that bisphosphonates have direct and indirect effects on tumor cells. However, as compared to inhibition of bone resorption, cytotoxic effects require much higher concentration (not practically achievable clinically) with potentially greater systemic toxicity.[3] The specific delivery of antineoplastic agents to bone tumor sites, exploiting bone-seeking properties of bisphosphonates, has been a target for many research projects over several decades.[4] Previously, a number of research groups had designed, synthesized, and tested bisphosphonate−antineoplastic drug conju-

* To whom correspondence should be addressed. Phone: +358-2-333 6770. Fax: +358-2-333 6776.
[†] University of Turku.
[‡] MBC Pharma Inc.

10.1021/jo800317e CCC: $40.75 © 2008 American Chemical Society
Published on Web 05/13/2008

gates.[5] The cytotoxic drugs, methotrexate, melphalan, doxorubicin, or *cis*-platinin, were directly covalently attached to the terminal amino group of bisphosphonate, pamidronate (**1b**). However, the anticancer properties of these conjugates tested in certain animal models proved to be encouraging but far from perfect and, in the case of doxorubicin, even negative.[5b] Unfortunately, no data were presented on the stability of these conjugates and the kinetics of accumulation in the bone. Thus, it is possible that the covalent bond between the components of the conjugates was either too stable or too unstable in vivo to provide the desired concentrations of a cytotoxic compound in bone. Most likely, intact, negatively charged conjugates with a stable covalent bond would not be able to interact effectively with intracellular molecular targets. On the other hand, an unstable bond would cleave in the blood stream and could not provide a sufficient increase of the active compound at bone tissues. Recently it has been suggested that bisphosphonates covalently linked via a phosphate group to cytotoxic agents, such as structurally modified nucleosides provide an optimal stability. This linkage allows the intact conjugate to survive in the circulation, bind the mineral matrix of bone, and subsequently release both drugs in the bone microenvironment.[6] Compounds designed in such a way will localize at the site of tumor cell induced bone destruction and combine antiresorptive and antitumor activities. These conjugates may become promising drugs that would increase the local concentration of the cytotoxic agent, greatly improving efficacy without increasing systemic toxicity of chemotherapeutic.

To learn more about the physicochemical properties and serum stability of nucleoside bisphosphonate conjugates, a quantitative kinetic investigation of the hydrolytic reactions of nucleoside 5′-β,γ-methylene and 5′-β,γ-(1-hydroxyethylidene) triphosphates has been carried out over a wide pH range at elevate temperature and under physiological conditions in the presence and absence of Mg^{2+} and Ca^{2+} ions. In addition, the hydrolytic stability in human and mouse serum and the affinity toward hydroxyapatite have been investigated. The compounds studied include two conjugates of etidronate (**2**), viz. 5′-β,γ-(1-hydroxyethylidene) triphosphates of 5-fluorouridine (**4**) and *ara*-cytidine (**6**), and two conjugates of medronate (**3**), viz. 5′-β,γ-methylene triphosphates of 5-fluorouridine (**5**) and *ara*-cytidine (**7**) (Chart1).

CHART 1

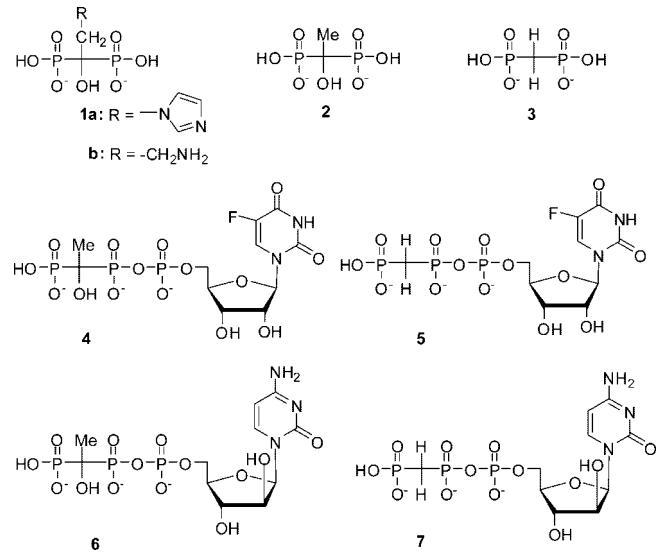

Results

Product Distribution of the Hydrolysis of 4−7. First-order rate constants for the hydrolysis of the bisphosphonate analogues of 5-fluorouridine and *ara*-cytidine 5′-triphosphates (**4**−**7**) were determined over a wide pH range (from pH 1.0 to 8.5, $I = 1.0$ mol L^{-1} with NaCl) at 90 °C by analyzing the compositions of the aliquots withdrawn at appropriate time intervals from the reaction mixture by RP HPLC. Each reaction mixture contained EDTA (2 mmol L^{-1}) to suppress possible metal ion catalysis. The products were characterized either by spiking with authentic samples or by mass spectrometric analysis (HPLC/ESI-MS). Over the pH range studied, disappearance of the starting material was accompanied by formation of the corresponding nucleoside 5′-monophosphate, viz. 5-fluorouridine 5′-monophosphate (**8**) from **4** and **5** and *ara*-cytidine 5′-monophosphate (**9**) from **6** and **7** (Scheme 1). With the β,γ-(1-hydroxyethylidene) analogues (**4**, **6**), the starting material was entirely converted to the corresponding monophosphate (**4** to **8** and **6** to **9**) before any other products appeared. For example, the first-order rate constant for the hydrolysis of **6** to **9** was $(1.14 \pm 0.07) \times 10^{-2}$ s^{-1} at pH 7.5, while the first-order rate constant for the disappearance of **9** was $(3.4 \pm 0.2) \times 10^{-7}$ s^{-1}. The latter reaction proceeded by two parallel routes, viz. dephosphorylation to *ara*-cytidine (**10**, 15%) and deamination to *ara*-uridine 5′-monophosphate (**11**, 85%). The methylene analogues (**5** and **7**) did not, in turn, demonstrate quantitative accumulation of monophosphate prior to the formation of secondary products. Dephosphorylation to nucleoside, either 5-fluorouridine (**12**) or *ara*-cytidine (**10**), was clearly visible at the late stage of the hydrolysis, but the maximum time-dependent concentration of the monophosphate still was more than 90%. The situation was more complicated only under mildly acidic conditions (pH 3−6) and only with **7**. In addition to *ara*-cytidine 5′-monophosphate (**9**), two other products accumulated, as shown by the time-dependent product distribution in Figure 1. In parallel to formation of 5′-monophosphate **9**, the starting material was deaminated to *ara*-uridine 5′-β,γ-methylenetriphosphate (**13**), as indicated by the m/z $[M - H]^-$ 481.2 and the UV absorption

(1) (a) Coleman, R. E. *Clin. Cancer Res.* **2006**, *12*, 6243s–6249s. (b) Body, J.-J. *Supportive Care Cancer* **2006**, *14*, 408–418. (c) Lipton, A.; Berenson, J. R.; Body, J. J.; Boyce, B. F.; Bruland, O. S.; Carducci, M. A.; Cleeland, C. S.; Clohisy, D. R.; Coleman, R. E.; Cook, R. J.; Guise, T. A.; Pearse, R. N.; Powles, T. J.; Rogers, M. J.; Roodman, G. D.; Smith, M. R.; Suva, L. J.; Vessella, R. L.; Weilbaecher, K. N.; King, L. *Clin. Cancer Res.* **2006**, *12*, 6209s–6212s.

(2) (a) Body, J. J.; Diel, I.; Bell, R. *Semin. Oncol.* **2004**, *31*, 73–78. (b) Cameron, D. *Semin. Oncol.* **2004**, *31*, 79–82. (c) Picket, F. A. *J. Dent. Hyg.* **2006**, *80*, 10. (d) Sanna, G.; Preda, L.; Bruschini, R.; Rocca, M. C.; Ferretti, S.; Adamoli, L.; Verri, E.; Franceschelli, L.; Goldhirsch, A.; Nole, F. *Ann. Oncol.* **2006**, *17*, 1512–16.

(3) (a) Daubine, F.; Le Gall, C.; Gasser, J.; Green, J.; Clezardin, P. *J. Natl. Cancer Inst.* **2007**, *99*, 322–330. (b) Clezardin, P.; Ebetino, F. H.; Fournier, P. G. *Cancer Res.* **2005**, *65*, 4971–4974. (c) Green, J. R. *Oncologist* **2004**, *9*, 3–13. (Suppl. 4)

(4) For reviews see: (a) Uludag, H. *Curr. Pharm. Des.* **2002**, *8*, 1929–1944. (b) Hirabayashi, H.; Fujisaki, J. *Clin. Pharmacokinet.* **2003**, *42*, 1319–30.

(5) (a) Hosain, F.; Spencer, R. P.; Couthon, H. M.; Sturtz, G. L. *J. Nucl. Med.* **1996**, *37*, 105–107. (b) Sturtz, G. A.; Appere, G. A.; Breistol, K. A.; Fodstad, O. A.; Schwartsmann, G.; Hendriks, H. R. *Eur. J. Med. Chem.* **1992**, *27*, 825–833. (c) Sturtz, G. L.; Couthon, H. M.; Fabulet, O.; Mian, M. A.; Rosini, S. *Eur. J. Med. Chem.* **1993**, *28*, 899–903. (d) Fabulet, O.; Sturtz, G. A. *Phosphorus Sulfur Silicon Relat. Elem.* **1995**, *101*, 225–234.

(6) (a) Karpeisky, M. Y.; Padyukova, N. S.; Mikhailov, S. N.; Dixon, H. B. F.; Tzeitline, G. US patent 6,214,812 B1. (MBC Research, Inc., Boulder, CO, 2001). (b) Karpeisky, M. Y.; Padyukova, N. S.; Mikhailov, S. N.; Dixon, H. B. F.; Tzeitline, G. US patent 6,750,340 B2(MBC Research, Inc., Boulder, CO, 2004). (c) Reinholz, G. G.; Getz, B.; Sanders, E. S.; Karpeisky, M. Y.; Padyukova, N. S.; Mikhailov, S. N.; Ingle, J. N.; Spelsberg, T. C. *Breast Cancer Res. Treat.* **2002**, *71*, 257–268.

SCHEME 1

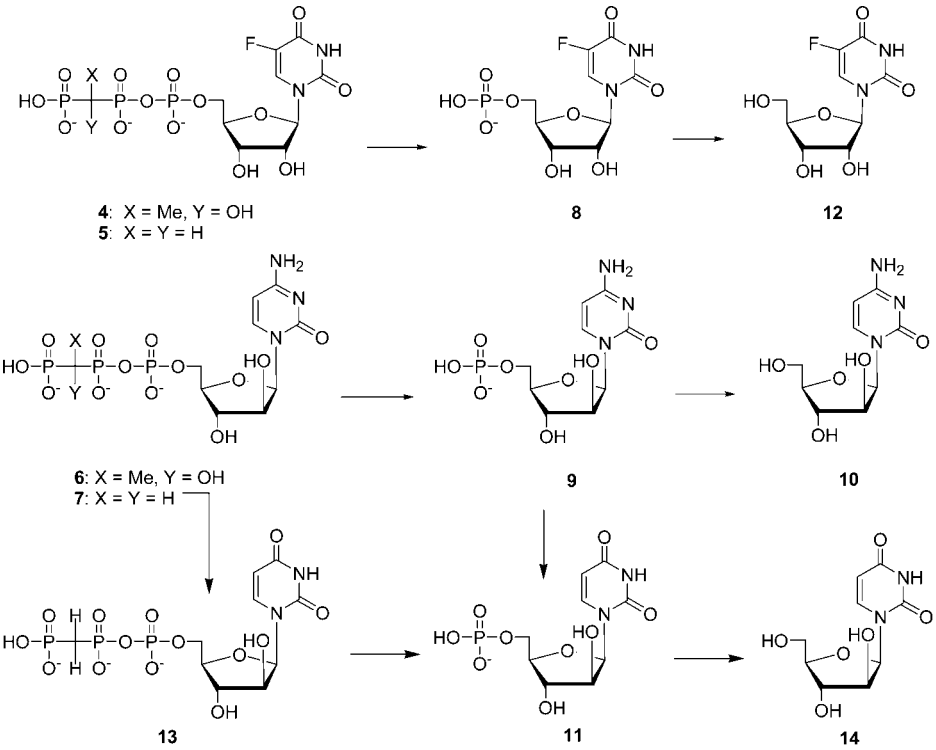

maximum 262 nm of the HPLC signal of this product at t_R = 4.0 min (eluent 0.1 mol L^{-1} aq KH_2PO_4, flow rate 1.0 mL min^{-1}). This product, as well as the *ara*-cytidine 5′-monophosphate (**9**), was then slowly converted to *ara*-uridine 5′-monophosphate (**11**), exhibiting t_R = 6.5 min, *m*/*z* $[M + H]^+$ 325.4, and UV absorption maximum 262 nm.

pH−Rate Profiles for the Hydrolysis of 4−7. The pH−rate profiles for the hydrolysis of **4**−**7** at 90 °C (I = 1.0 mol L^{-1}) are depicted in Figure 2 and the numerical values of the rate constants are listed in Table 1. The rate constants were usually obtained at only one buffer concentration, but the contribution of buffer catalysis may in all likelihood be neglected, since the rate constants obtained at pH 4 at the buffer concentrations of 0.05 and 0.2 mol L^{-1} were identical within the limits of experimental errors.

As seen, the β,γ-(1-hydroxyethylidene) derivatives, **4** and **6**, are hydrolyzed over the whole pH range studied, i.e., from pH 1.0 to 8.5, approximately as rapidly. Evidently the base moiety does not participate in the hydrolysis of these compounds. The reaction is first order in hydroxide ion concentration at pH >6 and the rate levels off to a constant value upon approaching pH 8, which suggests that the starting materials undergo a kinetically significant deprotonation around pH 7.5. The situation

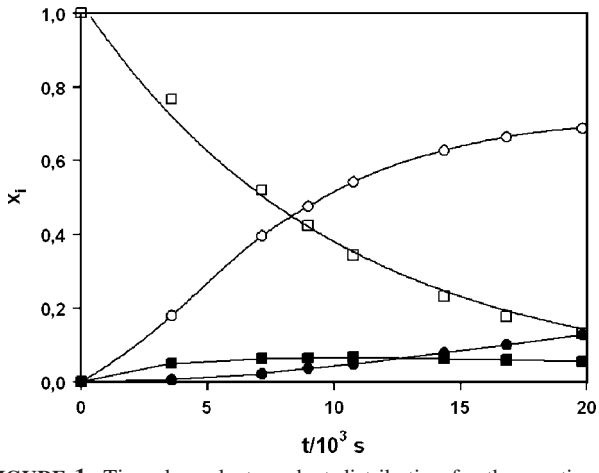

FIGURE 1. Time-dependent product distribution for the reaction of *ara*-cytidine 5′-β,γ-methylene triphosphate (**7**) at pH 4 and 90 °C. Notation: (□) **7**, (■) *ara*-cytidine 5′-monophosphate (**9**), (●) *ara*-uridine 5′-monophosphate (**11**), and (○) *ara*-uridine 5′-β,γ-methylene triphosphate (**13**). The pH was adjusted with HEPES buffer (0.05 mol L^{-1}) and the ionic was maintained at 1.0 mol L^{-1} with sodium chloride and the concentration of EDTA at 2 mmol L^{-1}.

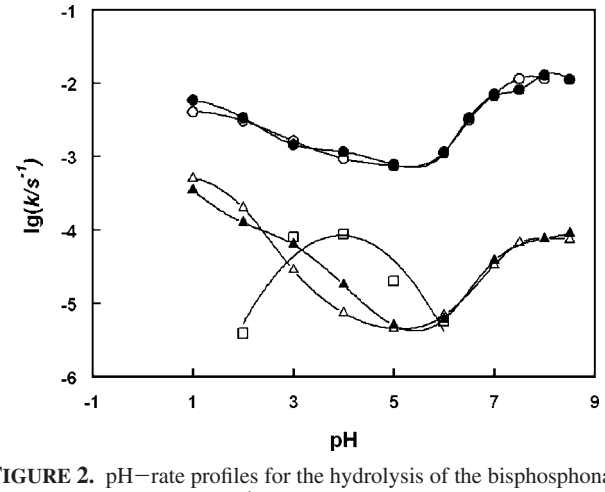

FIGURE 2. pH−rate profiles for the hydrolysis of the bisphosphonate analogues of nucleoside 5′-triphosphates (**4**−**7**) to nucleoside 5′-monophosphates (**8**, **9**). Notation: 5-fluorouridine 5′-β,γ-(1-hydroxyethylidene) triphosphate (**4**, ●), *ara*-cytidine 5′-β,γ-(1-hydroxyethylidene) triphosphate (**6**, ○), 5-fluorouridine 5′-β,γ-methylene triphosphate (**5**, Δ), *ara*-cytidine 5′-β,γ-methylene triphosphate (**7**, ▲). Open squares (□) refer to the deamination of **7**. (T = 90 °C, I = 1.0 mol L^{-1} with NaCl, [EDTA] = 2 mmol L^{-1}.)

TABLE 1. First-Order Rate Constants for the Hydrolysis of 5-Fluorouridine 5′-β,γ-(1-Hydroxyethylidene) Triphosphate (4) and 5′-β,γ-Methylene Triphosphate (5) to 5-Fluorouridine 5′-Monophosphate (8) and the Hydrolysis of *ara*-Cytidine 5′-β,γ-(1-Hydroxyethylidene) Triphosphate (6) and 5′-β,γ-Methylene Triphosphate (7) to *ara*-Cytidine 5′-Monophosphate (9) at 90 °C (I = 1.0 mol L^{-1} with NaCl; [EDTA] = 2 mmol L^{-1})

		$k/10^{-4}$ s^{-1}			
pH	solution	**4**	**6**	**5**	**7**
1.0	0.1 mol L^{-1} HCl	58.5 ± 1.3	41.1 ± 1.8	4.65 ± 0.23	3.45 ± 0.06
2.0	0.01 mol L^{-1} HCl	33.5 ± 0.9	31.2 ± 0.7	1.66 ± 0.03	1.31 ± 0.02
3.0	0.05 mol L^{-1} (HCOOH/HCOONa)	14.5 ± 0.6	16.4 ± 3.0	0.279 ± 0.008	1.35 ± 0.08[a]
4.0	0.05 mol L^{-1} (HOAc/NaOAc)	11.40 ± 0.7	9.32 ± 0.09	0.074 ± 0.002	1.09 ± 0.03[a]
5.0	0.05 mol L^{-1} (HOAc/NaOAc)	7.68 ± 0.06	7.34 ± 0.08	0.043 ± 0.001	0.248 ± 0.001[a]
6.0	0.05 mol L^{-1} (HEPES)	11.3 ± 0.2	11.6 ± 0.4	0.068 ± 0.002	0.115 ± 0.001[a]
6.5	0.05 mol L^{-1} (HEPES)	33.5 ± 1.1	31.3 ± 1.1		
7.0	0.05 mol L^{-1} (HEPES)	67.2 ± 1.2	70.9 ± 1.1	0.330 ± 0.002	0.400 ± 0.009
7.5	0.05 mol L^{-1} (Glycine)	82.0 ± 3.0	114 ± 7	0.664 ± 0.032	
8.0	0.05 mol L^{-1} (Glycine)	128 ± 3	115 ± 4	0.755 ± 0.057	0.763 ± 0.049
8.5	0.05 mol L^{-1} (Glycine)	111 ± 4		0.740 ± 0.029	0.883 ± 0.043

[a] At pH 3−6, the predominant reaction of **7** is deamination of the starting material to *ara*-uridine 5′-(β,γ-methylene) triphosphate (**13**). This reaction is at pH 5 3.6 times as fast as the phosphate hydrolysis.

is less clear on going from pH 6 to more acidic solutions. The hydrolysis becomes oxonium ion catalyzed at pH <5, but the reaction order in oxonium ion concentration is clearly less than unity. Even around pH 1, where the rate reaches a plateau value, the hydrolysis still is slower than at pH 8. Evidently several kinetically significant protolytic equilibria overlap in the pH range 1−5.

The β,γ-methylene triphosphate analogues, **5** and **7**, are hydrolytically considerably more stable than their β,γ-(1-hydroxyethylidene) counterparts discussed above. The stability difference ranges from 1 order of magnitude to more than 2 orders of magnitude. As with the β,γ-(1-hydroxyethylidene) analogues, the cleavage of **5** and **7** is clearly first order in hydroxide ion concentration at pH 6−7 and reaches a plateau value upon approaching pH 8. At pH <4, the hydrolysis of **5** is approximately first order in oxonium ion concentration. With **7**, the situation is more complicated. As discussed above, this compound undergoes hydrolytic deamination of the cytosine base. For this reason, the overall hydrolytic stability is at pH 3−6, much lower than that of **5**, having a 5-fluorouracil base. The phosphate hydrolysis, which occurs as a minor side reaction, is first order in oxonium ion concentration (and slightly faster than that of **5**) at pH 3−5, turns pH independent on passing pH 3, and is again acid-catalyzed at pH <2.

^{18}O Incorporation and Temperature Dependence. To clarify whether the hydrolysis to nucleoside 5′-monophosphates proceeds by the rupture of the P(α)−O or P(β)−O bond, **6** and **7** were hydrolyzed in ^{18}O-enriched water at pH 8.0 (90 °C) and the nucleoside monophosphate product, **9**, was analyzed by HPLC-ESI-MS. No incorporation of ^{18}O into **9** was observed in either case. Accordingly, the hydrolysis proceeds by cleavage of the P(β)−O bond.

The dependence of the hydrolysis rate of **4**−**7** on temperature was studied at pH 5, a pH where the reaction is almost pH independent. Table 2 records the rate constants obtained at 10 °C intervals in the range from 50 to 90 °C with **4** and **6**, and from 60 to 90 °C with **5** and **7**. Extrapolation to physiological temperature by the Arrhenius equation indicates that the half-lives of the hydrolysis of the β,γ-(1-hydroxyethylidene) phosphonates, **4** and **6**, at 37 °C are 62 ± 5 and 50 ± 20 h, respectively. For comparison, the half-lives for the same compounds at pH 7.4, i.e. at the upper plateau, are 16 and 12 h at 37 °C (I = 0.14 mol L^{-1} with NaCl). The β,γ-methylene phosphonates, **5** and **7**, are hydrolyzed at pH 5 so slowly that reliable extrapolation to physiological temperature is not possible. At pH 7.4, the half-lives are 2400 and 1100 h for the hydrolysis of **5** and **7**, respectively.

TABLE 2. First-Order Rate Constants for the Hydrolysis of 5-Fluorouridine 5′-β,γ-(1-Hydroxyethylidene) Triphosphate (4) and 5′-β,γ-Methylene Triphosphate (5) to 5-Fluorouridine 5′-Monophosphate (8) and the Hydrolysis of *ara*-Cytidine 5′-β,γ-(1-Hydroxyethylidene) Triphosphate (6) to *ara*-Cytidine 5′-Monophosphate (9) at Different Temperatures at pH 5.0 (0.05 mol L^{-1} AcOH/AcONa buffer; I = 1.0 mol L^{-1} with NaCl)[a]

	$k/10^{-6}$ s^{-1}			
T/°C	**4**	**6**	**5**	**7**
50.0	13.9 ± 0.6	15.1 ± 0.7		
60.0	42.4 ± 0.9	46.1 ± 4.5	0.188 ± 0.003	3.63 ± 0.02
70.0	129 ± 6	135 ± 7	0.763 ± 0.018	7.19 ± 0.08
80.0	320 ± 10	327 ± 11	2.32 ± 0.04	15.9 ± 0.1
90.0	768 ± 6	734 ± 8	4.43 ± 0.15	24.8 ± 0.1

[a] The rate constants given for *ara*-cytidine 5′-β,γ-methylene triphosphate (**7**) refer to the disappearance of the starting material, including contributions of deamination and phosphate hydrolysis.

The enthalpies and entropies of activation for the hydrolysis of the β,γ-(1-hydroxyethylidene) phosphonates (**4** and **6**) are at pH 5.0 quite similar: for **4** $\Delta H^{\ddagger}$ = (95 ± 2) kJ mol^{-1} and $\Delta S^{\ddagger}$ = −(44 ± 5) J K^{-1} mol^{-1}, and for **6** $\Delta H^{\ddagger}$ = (92 ± 2) kJ mol^{-1} and $\Delta S^{\ddagger}$ = −(53 ± 6) J K^{-1} mol^{-1}. The markedly slower hydrolysis of the β,γ-methylene phosphonates is of enthalpic origin, the activation parameters obtained with **5** being: $\Delta H^{\ddagger}$ = (116 ± 4) kJ mol^{-1} and $\Delta S^{\ddagger}$ = −(25 ± 10) J K^{-1} mol^{-1}. With **7**, deamination predominates at pH 5 and, hence, activation parameters for the phosphate hydrolysis cannot be reliably determined.

The Effect of Mg^{2+} and Ca^{2+}on the Hydrolysis of 4−7. The effect of Mg^{2+} and Ca^{2+} on the hydrolysis of **4**−**7** was studied under modeled physiological conditions (pH 7.4; T = 37 °C; I = 0.14 mol L^{-1} with NaCl). The time-dependent product distribution under these conditions differs from that at 90 °C in the sense that the accumulation of the nucleoside 5′-monophosphate (**8** or **9**) is not quantitative, but hydrolysis of the starting material to nucleoside 5′-phosphate is followed by dephosphorylation to nucleoside. While the monophosphate accumulation still is almost quantitative with the β,γ-(1-hydroxyethylidene) phosphonate derivatives (**4**, **6**) (Figure 3), the appearance of 5′-monophosphates during the hydrolysis of the more stable β,γ-methylene analogues (**5**, **7**) is barely

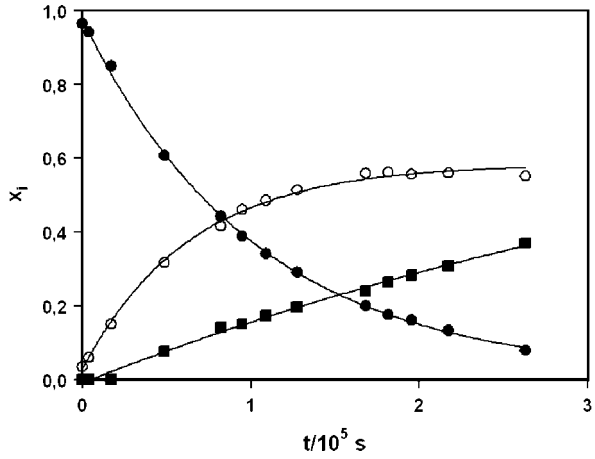

FIGURE 3. Time-dependent product distribution for the reaction of 5-fluorouridine 5′-β,γ-(1-hydroxyethylidene) triphosphate (**4**) at pH 7.4 and 37 °C in the presence of Mg^{2+} (0.1 mmol L^{-1}). The pH was adjusted with a HEPES buffer and the ionic was maintained at 0.14 mol L^{-1} with NaCl. Notation: **4** (●), 5-fluorouridine 5′-monophosphate (**8**, ○), and 5-fluorouridine (**12**, □).

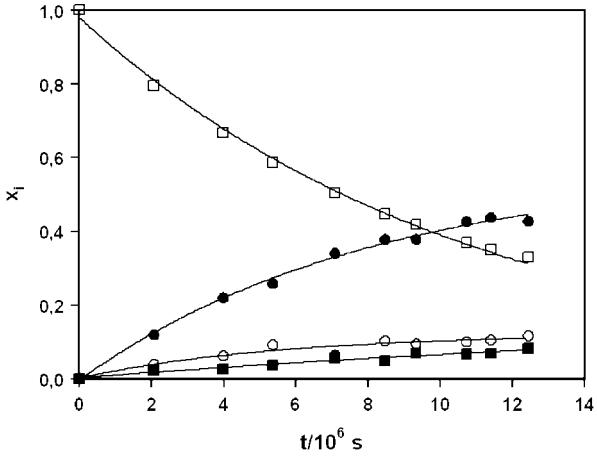

FIGURE 4. Time-dependent product distribution for the reaction of *ara*-cytidine 5′-β,γ-methylene triphosphate (**7**) at pH 7.4 and 37 °C in the presence of Mg^{2+} (2.0 mmol L^{-1}). The pH was adjusted with HEPES buffer and the ionic was maintained at 0.14 mol L^{-1} with NaCl. Notation: **7** (□), *ara*-cytidine 5′-monophosphate (**9**, ■), *ara*-uridine (**14**, ●), and *ara*-cytidine (**10**, ○).

noticeable. Among the hydrolysis products of **5**, 5-fluorouracil was observed in addition to 5-fluorouridine (**12**) and its monophosphate (**8**). In other words, 5-fluorouridine and possibly also **5** itself underwent hydrolysis to 5- fluorouracil. Hydrolysis of **7** gave *ara*-uridine as the main product (Figure 4). In addition, *ara*-cytidine (**10**) and *ara*-cytidine 5′-monophosphate (**9**) were formed. Deaminated starting material, the 5′-β,γ-methylene triphosphate of *ara*-uridine (**13**), appeared as an intermediate, but at a very low level (1−2%), and only traces of *ara*-uridine 5′-monophosphate (**11**) could be detected at any stage of the reaction.

Table 3 summarizes the rate constants obtained for the disappearance of **4**−**7** in the presence of Mg^{2+} (≤2 mmol L^{-1}) and Ca^{2+} (≤50 mmol L^{-1}) ions. With the β,γ-(1-hydroxyethylidene) triphosphate analogues (**4**, **6**), hydrolysis to the 5′-monophosphates (**8** or **9**) is somewhat retarded by both Mg^{2+} and Ca^{2+}, and, hence, intermediary accumulation of these compounds is diminished. Previously[5] published results show that Mg^{2+} and Ca^{2+} do not noticeably accelerate the dephosphorylation. Hydrolysis of the β,γ-methylene triphosphate analogues (**5**, **7**) is slightly retarded by Mg^{2+}, but accelerated by Ca^{2+}. Acceleration of the cleavage by Ca^{2+} was accompanied by diminution of the proportion of deamination to *ara*-uridine.

TABLE 3. First-Order Rate Constants for the Cleavage of 4−7 in the Presence of Mg^{2+} and Ca^{2+} Ions at 37 °C and pH 7.4 (I = 0.14 mol L^{-1} with NaCl)

compd	$[Mg^{2+}]$/ mmol L^{-1}	$k/10^{-6}$ s^{-1}	$[Ca^{2+}]$/ mmol L^{-1}	$k/10^{-6}$ s^{-1}
4	none	12.4 ± 0.17		
	0.1	9.31 ± 0.088	2.0	6.48 ± 0.061
	1	5.08 ± 0.096	10.0	3.68 ± 0.023
	2	5.47 ± 0.043	50.0	3.05 ± 0.026
6	none	15.7 ± 0.286		
	0.1	11.8 ± 0.170	2.0	7.60 ± 0.051
	1.0	7.40 ± 0.049	10.0	4.30 ± 0.038
	2.0	6.23 ± 0.066	50.0	3.57 ± 0.043
5	none	0.09 ± 0.005		
	0.1		2.0	0.09 ± 0.004
	1.0	0.08 ± 0.003	10.0	0.12 ± 0.005
	2.0	0.06 ± 0.001	50.0	0.19 ± 0.005
7	none	0.20 ± 0.004		
	0.1	0.16 ± 0.004	2.0	0.11 ± 0.004
	1.0	0.11 ± 0.003	10.0	0.18 ± 0.007
	2.0	0.09 ± 0.002	50.0	0.14 ± 0.095

TABLE 4. Half-Lives for the Hydrolysis of 5-Fluorouridine 5′-β,γ-(1-Hydroxyethylidene) Triphosphate (4) and 5′-β,γ-Methylene Triphosphate (5) to 5-Fluorouridine 5′-Monophosphate (8) and the Hydrolysis of *ara*-Cytidine 5′-β,γ-(1-Hydroxyethylidene) Triphosphate (6) and 5′-β,γ-Methylene Triphosphate (7) to *ara*-Cytidine 5′-Monophosphate (9) in Human and Mouse Serum at 37 °C

	$t_{1/2}$/ h	
compd	human serum	mouse serum
4	3.5	17.4
5	2.9	0.4
6	5.7	33
7	2.4	0.3

Kinetic Measurements in Human and Mouse Serum. The hydrolytic stability of **4**−**7** was additionally determined in human and mouse serum. In each case, the disappearance of the starting material obeyed first-order kinetics. Table 4 records the half-lives observed. The product distribution was quite similar to that in aqueous buffers. In other words, the predomi-

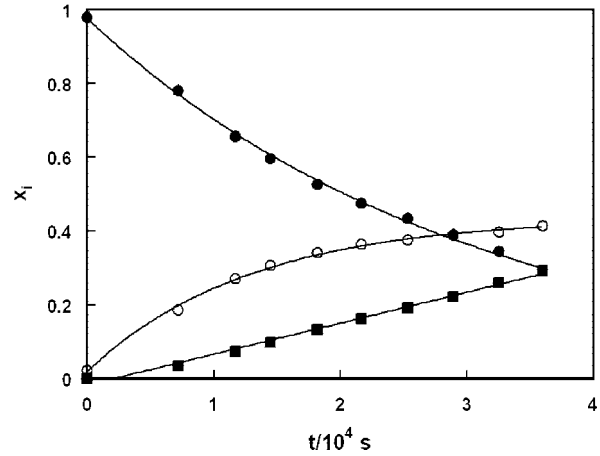

FIGURE 5. Time-dependent product distribution for the reaction of *ara*-cytidine 5′-β,γ-(1-hydroxyethylidene) triphosphate (**6**) in human serum at 37 °C. Notation: **6** (●), *ara*-cytidine 5′-monophosphate (**9**, ○), and *ara*-cytidine (**10**, □).

TABLE 5. Elution Times of Various Phosphate and Phosphonate Compounds on a Hydroxyapatite Column (Bio-Scale CHT10-I, 12 mm × 88 mm) with Elution with a 1.5 mol L^{-1} and 0.5 mol L^{-1} Sodium Phosphate Buffer at a Flow Rate of 2 mL min^{-1}

	t_R/min				
	1.5 mol L^{-1} buffer			0.5 mol L^{-1} buffer	
compd	pH 5.8	pH 6.8	pH 7.8	pH 6.8	RP-column[a]
4	5.5	6.0	6.6	17.7	4.1
6	5.5	5.9	6.8	20.3	3.4
5	3.9	3.8	3.9	6.1	3.9
7	3.8	3.7	3.8	6.1	3.3
5′-UMP	3.3	3.4	3.5	4.3	5.2
5′-UDP	3.4	3.5	3.4		2.8
5′-UTP	3.7	3.7	3.6		3.6
oligodeoxynucleotide	2.6	2.5	2.6		12.7[b]
zoledronate	24.6	17.4	14.9		2.9

[a] Atlantis C18 column (4.6 × 250 mm, 5 μm), isocratic elution (1 mL min^{-1}) with potassium phosphate buffer (0.1 mol L^{-1}, pH 6.0), containing EDTA (2 mmol L^{-1}). [b] Refers to gradient elution from aq NH_4OAc (50 mmol L^{-1}) to a 1:1 mixture of aq NH_4OAc (50 mmol L^{-1}) and MeCN in 30 min. The sequence is 5′-TAA GTA GCG AAC ACC AAA GAT GAT AT-3′.

nant reaction was hydrolysis to nucleoside 5′-monophosphate. The time-dependent product distribution obtained with *ara*-cytidine 5′-β,γ-(1-hydroxyethylidene) triphosphate (**6**) in human serum is shown in Figure 5 as an example. In mouse serum, a small amount of an unidentified product was formed in addition to the nucleoside and nucleoside 5′-monophosphate. This product is formed mainly from nucleoside monophosphate and/or nucleoside. The amount remained below 5%, except with **4**, which gave it up to 10%. Otherwise the product distribution remained constant over the pH range studied. No depyrimidination was observed to take place.

Hydroxyapatite-Binding Affinities. The tendency of **4**−**7** to undergo adsorption to bone material was elucidated by determination of their elution times on a hydroxyapatite column (Bio-Scale CHT10-I, 12 mm × 88 mm). Compounds **4**−**7** were eluted with a 1.5 mol L^{-1} sodium phosphate buffer at three different pH values (pH 5.8, 6.8, and 7.8) at a flow rate of 2 mL min^{-1}. To verify that no structural changes took place during the elution, the eluted compounds were subjected to RP HPLC by coinjection with the original sample. The results are listed in Table 5.

Discussion

The phosphonate analogues, **4**−**7**, of nucleoside 5′-triphosphates studied are decomposed both in aqueous buffers and in human and mouse serum by departure of the pyrophosphonate moiety, i.e., by cleavage of the bond between α- and β-phosphoric acid residues. Over the whole pH range studied, the β,γ-(1-hydroxyethylidene) triphosphate analogues, **4** and **6**, react from 1 to more than 2 orders of magnitude faster than the β,γ-methylene triphosphate analogues, **5** and **7**. With both types of compounds, the hydrolysis turns from a hydroxide ion-catalyzed to a pH-independent reaction on passing pH 7. At pH >7, the predominant ionic form of the triphosphate moiety is a tetraanion. Since ^{18}O is not incorporated into the nucleoside monophosphate product when the hydrolysis is carried out in ^{18}O-enriched water, the solvent-derived nucleophile, either water or the hydroxide ion, must attack the β-phosphorus atom. Accordingly, three alternative mechanisms appear worth considering: (i) dissociative breakdown of the triphosphate tetraanion (reaction a in Scheme 2), (ii) attack of water on the triphosphate tetraanion (reaction b), or (iii) attack of hydroxide ion on the triphosphate trianion (reaction c).

SCHEME 2

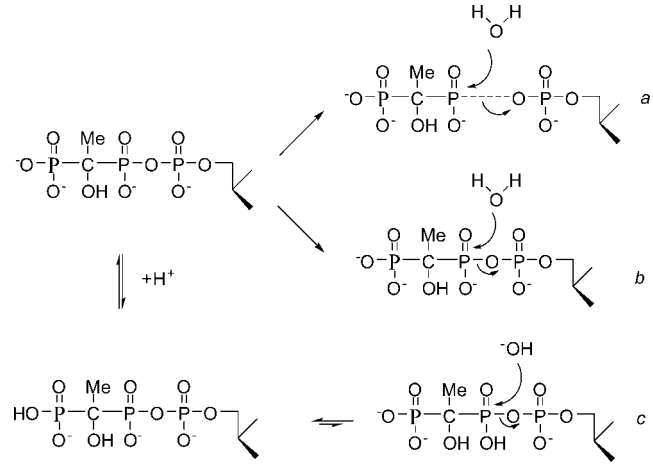

A dissociative mechanism is usually utilized only by phosphomonoesters, i.e., when formation of a metaphosphate-like intermediate, though preassociated with a molecule of water, is possible.[8] This is not possible upon cleavage of the P(β)−O bond and, hence, mechanistic alternative a in Scheme 2 appears less probable than alternative b or c, which may be either associative reactions giving a phosphorane intermediate or synchronous S_N2-type displacements. Extensive studies with 3′,5′-dinucleoside monophosphates and their phosphotriester counterparts have led to the conclusion that among the two kinetically equivalent mechanisms, viz. attack of either 2′-OH on deprotonated (monoanionic) phosphate or 2′-O^- on protonated (neutral) phosphate, the latter reaction is faster.[9] Although an analogous mechanism, viz. an attack of hydroxide ion on protonated (neutral) β-phosphate (reaction c in Scheme 2), cannot be strictly excluded, attack of water on anionic β-phosphate (reaction b in Scheme 2) appears, however, more attractive in this particular case. The vicinal hydroxyethylidene group may effectively hydrogen bond the negatively charged phosphate, facilitating the nucleophilic attack. The marked rate-accelerating effect of the carbon-bound hydroxy group may be attributed to stabilization of the phosphorane intermediate by hydrogen bonding to one of the oxygen atoms of the β-phosphate, as depicted in Scheme 3. The breakdown of this intermediate then proceeds by P(β)−O bond cleavage concerted with a water-mediated proton transfer from the phosporane hydroxyl ligand to the departing α-phosphate.

Two previous observations lend support to the significance of the intramolecular hydrogen bond stabilization described in Scheme 3. First, diribonucleoside-3′,3′-monophosphates undergo transesterification to nucleoside 2′,3′-monophosphate by attack of one of the 2′-OH groups on the phosphorus atom, followed by departure of the other 3′-linked nucleoside.[10] Methylation of one of the 2′-OH groups retards the reaction by a factor of 23 (when the statistic correction by a factor of 2 has been taken into account). Comparative measurements with tri(ribonucleoside)-3′,3′,5′-triphosphates has shown that the rate-accelerating effect of the 2′-OH of the departing nucleoside may be attributed to the stabilization of the intermediate rather than the leaving group by hydrogen bonding (as depicted by structure a in

(7) Kuusela, S.; Lönnberg, H. *J. Phys. Org. Chem.* **1993**, *6*, 347–356.

SCHEME 3

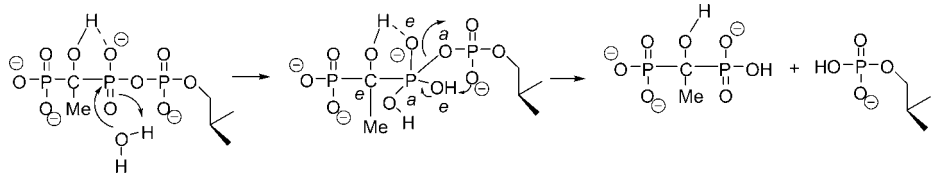

SCHEME 4

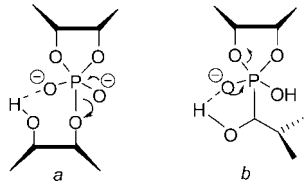

Scheme 4 for the diester): the departure of both the 3′-and 5′-linked nucleosides is accelerated as much.[11] Second, the internucleosidic 3′-O-P-CH(OH)-5′ linkage of a hydroxyphosphonate analogue of adenylyl-3′,5′-adenosine is isomerized to the corresponding 2′,5′-linkage considerably faster than its deoxy counterpart, 3′-O-P-CH_2-5′.[12] This acceleration has been attributed to stabilization of the mono- and dianionic phosphorane intermediates by intramolecular hydrogen bonding of the hydroxyl group to a phorphorus-bound oxyanion (structure *b* in Scheme 4). It is worth noting that this stabilization allows hydroxide ion-catalyzed isomerization via a dianionic phosphorane, the reaction which is otherwise not encountered, owing to the fact that a dianionic phosphorane is too unstable to pseudorotate. Evidently, kinetically invisible proton transfer between the carbon- and phosphorus-bound oxygens stabilizes the dianionic structure to such an extent that pseudoration becomes possible.

At pH 7.4, Mg^{2+} and Ca^{2+} ions at physiological concentrations retard the hydrolysis of the β,γ-(1-hydroxyethylidene) 5′-triphosphate analogues (**4**, **6**) by a factor of 2−4. Mg^{2+} also retards the hydrolysis of the 5′-β,γ-methylene triphosphates (**5**, **7**), while Ca^{2+} slightly accelerates the cleavage of these compounds. Since Mg^{2+} and Ca^{2+} ions do not noticeably accelerate the dephosphorylation,[7] the intermediary accumulation of the nucleoside 5′-monophosphate turns less quantitative, except with **5** and **7** in the presence of Ca^{2+}.

As shown in Figure 1, the hydrolysis of **4**−**7** is pH independent over a narrow pH range around pH 5, i.e., under the conditions where the predominant ionic form is trianion, the γ-phosphonate group being singly protonated. The pK_a value for the terminal monohydrogen phosphonate group in all likelihood is around 7.[13] Consistent with the preceding discussion, this reaction most likely proceeds by the nucleophlic attack of water (instead of hydroxide ion) on the β-phosphorus atom. The values for the entropy of activation of the hydrolysis of **4**−**7** are negative and, hence, consistent with the proposed associative nature of the reaction.

The decomposition of **4**−**7** becomes hydronium ion catalyzed at pH <5, but the apparent reaction order in oxonium ion concentration remains considerably below unity. Consistent with the preceding discussion, the reaction may be assumed to proceed, depending on pH, by an attack of water on the β-phosphorus atom of the dianionic, monoanionic, and possibly neutral phosphate/phosphonate moiety. The pK_a values of the terminal dihydrogen phosphonate moiety probably fall in the range 2−3, while conversion of the monoanion and the neutral forms takes place at pH <2.[13,14] Owing to the existence of the dianionic and monoanionic species in several tautomeric forms, the observed rate constant for the hydrolysis cannot be attributed to any single ionic species, but it refers to several parallel reactions, the contributions of which vary with pH. This also explains why the reaction order deviates markedly from unity.

As mentioned above, *ara*-cytidine 5′-β,γ-methylene triphosphate (**7**) undergoes at pH 3−5 deamination of the cytosine base in addition to departure of the bisphosphonate moiety. At pH 5, the deamination to uridine 5′-β,γ-methylene triphosphate (**13**) is considerably faster than hydrolysis to *ara*-cytidine 5′-monophosphate (**9**), the first order rate constants for the deamination and the hydrolytic departure of the bisphosphonate moiety being 2.5×10^{-5} and 6.9×10^{-6} s^{-1}, respectively, at 90 °C. Under these conditions, the deamination of **7** most likely proceeds by an attack of a molecule of water on C6 of the N3-protonated cytosine moiety resulting in saturation of the 5,6-double bond, which is followed by rapid hydrolysis of the amidine moiety and dehydration to uracil base (Scheme 5).[15] Participation of the 2′-OH by an intramolecular nucleophilic attack on the C6 atom, suggested for the alkaline cleavage of *ara*-cytidine,[16] appears less since the 2′-*O*-methylation of *ara*-cytidine has been shown to retard the deamination of *ara*-cytidine only by a factor of 3.[17] At least this participation is less marked than with *ara*-uridine, with which the 2′-*O*-methylation retards the breakdown by more than 2 orders of magnitude.

(8) (a) Grzyska, P. K.; Czyryca, P. G.; Purcell, J.; Hengge, A. C. *J. Am. Chem. Soc.* **2003**, *125*, 13106–13111. (b) Wilkie, J.; Gani, D. *J. Chem. Soc., Perkin Trans. 2* **1996**, 783–787. (c) Hengge, A. C.; Edens, W. A.; Elsing, H. *J. Am. Chem. Soc.* **1994**, *116*, 5045–5049. (d) Thatcher, G. R.; Kluger, R. *Adv. Phys. Org. Chem.* **1989**, *25*, 99–265. (e) Herschlag, D.; Jencks, W. P. *J. Am. Chem. Soc.* **1989**, *111*, 7579–7586. (f) Friedman, J. M.; Freeman, S.; Knowles, J. R. *J. Am. Chem. Soc.* **1988**, *110*, 1268–1275. (g) Buchwald, S. L.; Friedman, J. M.; Knowles, J. R. *J. Am. Chem. Soc.* **1984**, *106*, 4911–4916. (h) Guthrie, J. P. *Acc. Chem. Res.* **1983**, *16*, 122–129. (i) Westheimer, F. H. *Chem. Rev.* **1981**, *81*, 313–326. (j) Ramirez, F.; Marecek, J. F. *Pure Appl. Chem.* **1980**, *52*, 1021–1045. (k) Kirby, A. J.; Varvoglis, A. G. *J. Am. Chem. Soc.* **1967**, *89*, 415–423.

(9) (a) Mikkola, S.; Kosonen, M.; Lönnberg, H. *Curr. Org. Chem.* **2002**, *6*, 523–538. (b) Kosonen, M.; Lönnberg, H. *J. Chem. Soc., Perkin Trans. 2* **1995**, 1203–1209. (c) Kosonen, M.; Oivanen, M.; Lönnberg, H. *J. Org. Chem.* **1994**, *59*, 3704–3708.

(10) Kiviniemi, A.; Lönnberg, T.; Ora, M. *J. Am. Chem. Soc.* **2004**, *126*, 11040–11045.

(11) Lönnberg, T.; Korhonen, J. *J. Am. Chem. Soc.* **2005**, *127*, 7752–7758.

(12) Lönnberg, T.; Kralikova, S.; Rosenberg, I.; Lönnberg, H. *Collect. Czech. Chem. Commun.* **2006**, *71*, 859–870.

(13) (a) Freedman, L. D.; Doak, G. O. *Chem. Rev.* **1957**, *57*, 479–523. (b) Solinova, V.; Kasicka, V.; Koval, D.; Cesnek, M.; Holy, A. *Electrophoresis* **2006**, *27*, 1006–1019.

(14) (a) Sajadi, S. A. A.; Song, B.; Gregan, F.; Siegel, H. *Inorg. Chem.* **1999**, *38*, 439–448. (b) Siegel, H.; Hofstetter, F.; Martin, R. B.; Milburn, R. M.; Scheller-Krattiger, V.; Scheller, K. H. *J. Am. Chem. Soc.* **1984**, *106*, 7935–7946.

(15) Kusmierek, J.; Käppi, R.; Neuvonen, K.; Shugar, D.; Lönnberg, H. *Acta Chem. Scand.* **1989**, *43*, 196–202.

(16) Notari, R. E.; Chin, M. L.; Wittebort, R. *J. Pharm. Sci.* **1972**, *61*, 1189–1195.

(17) Lönnberg, H.; Suokas, P.; Käppi, R.; Darzynkiewicz, E. *Acta Chem. Scand.* **1986**, *B40*, 798–805.

SCHEME 5

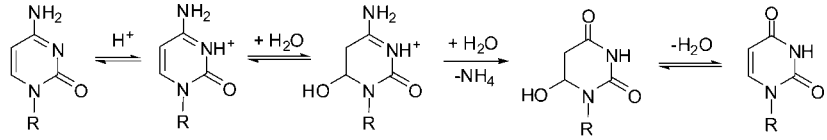

Under the modeled physiological conditions (pH 7.4, T = 37 °C, $[Mg^{2+}]$ = 2 mmol L^{-1}, I = 0.14 mol L^{-1} with NaCl), *ara*-uridine (**14**) is obtain as the main product, while its potential deaminated precursors, *ara*-uridine 5′-(β,γ-methylene) triphosphate (**13**) and 5′-monophosphate (**11**), appear only at low steady state level (<2%) during a kinetic run. *ara*-Cytidine (**10**) is formed as a minor product (25% of **14**). The fact that **10** and **14** seem to be formed in parallel rather than consecutively (Figure 4) suggests that **14** is formed via **13** and **11**, and possibly via **9** and **11**, not via **9** and **10** (Scheme 1).

Compounds **4**−**7** are hydrolyzed in human and mouse serum to nucleoside 5′-phosphates. The striking difference with hydrolysis in buffers is that the 5′-β,γ-methylene triphosphate analogues are in mouse serum exceptionally labile: **5** and **7** are hydrolyzed 5000 and 3000 times as fast as in buffer, respectively, suggesting their ability to act as substrate for degradative enzymes. In human serum, the acceleration is more modest: 700- and 400-fold with **5** and **7**, respectively. In striking contrast to the situation in buffers mimicking physiological conditions, deamination does not detectably compete with the phosphate hydrolysis. 5′-β,γ-(1-Hydroxyethylidene) triphosphates (**4**, **6**), which in physiological buffers are much more labile that their β,γ-methylene triphosphate counterparts, do not exhibit a similar increase in hydrolysis rate on going from buffers to serum. Their stability in mouse serum is comparable to the stability in buffer (pH 7.4) and a 2- to 4-fold increase in the hydrolysis rate takes place on going to human serum. Accordingly, the 1-hydroxyethylidene derivatives are in human serum slightly more stable than their methylene counterparts and in mouse serum the stability difference is 40- to 100-fold.

Experimental Section

Materials. Preparation of compounds **4**−**7** used in kinetic measurements has been described previously.[6,18]

Kinetic Measurements. The reactions were carried out in sealed tubes immersed in a thermostated water bath (90.0 ± 0.1 or 37.0 ± 0.1 °C). The oxonium ion concentration of the reaction solutions was adjusted with hydrogen chloride, sodium hydroxide and formate, acetate, *N*-[2-hydroxyethyl]piperazine-*N*-[2-ethanesulfonic acid] (HEPES), and glycine buffers. The oxonium ion concentrations of the buffer solutions were calculated with the aid of the known pK_a values of the buffer acids under the experimental conditions. Low buffer concentration was used (50 mmol L^{-1}). The initial substrate concentration was ca. 0.15 mmol L^{-1}. The composition of the samples withdrawn at appropriate intervals was analyzed on an Aquasil C18 column (4 × 150 mm, 5 μm), using a mixture of KH_2PO_4 (0.050 mol L^{-1}) and 0.1% MeCN. The observed retention times (t_R/min) for starting materials were 1.7 (**4**), 1.7 (**5**), 1.5 (**6**), and 1.8 (**7**) and retention times (t_R/min) for the hydrolysis products were 3.1 (**8**), 2.6 (**9**), 3.1 (**11**), and 2.0 (**13**). In the presence of metal ions and in serums, the decomposition of starting material was followed by an Atlantis C18 column (4.6 × 250 mm, 5 μm), using 0.1 mol L^{-1} KH_2PO_4 with 2 mM EDTA as an eluent. Signals were recorded on a UV-detector at a wavelength of 270 nm. The observed retention times (t_R/min^{-1}) for the products on RP HPLC (flow rate was 1 mL min) were 4.0 (**13**), 4.7 (**9**), 6.4 (**11**), 6.5 (**8**), 9.2 (5-F-Ura), 17.5 (**10**), 29.0 (**14**), and 30.0 (**12**). The observed retention times (t_R/min) for starting materials were 6.3 (**4**), 3.8 (**5**), 3.3 (**6**), and 3.4 (**7**). The reaction products were identified by the mass spectra (LC/MS). Aqueous ammonium acetate (5 mmol L^{-1}) was used as an eluent. The contribution of the buffer catalysis to the observed rate constants was insignificant even at the higher buffer concentration employed (0.2 mol L^{-1}).

Calculation of the Rate Constants. The pseudo-first-order rate constants for the decomposition of starting materials were obtained by applying the integrated first-order rate equation to the time-dependent diminution of the HPLC peak area of the starting material.

Mineral Binding. The mineral-binding properties of various phosphonate and phosphate compounds were followed by HPLC on a hydroxyapatite column (Bio-Scale CHT10-1, 12 mm × 88 mm); 1.5 mol L^{-1} potassium phosphate buffers (pH 5.8, 6.8, and 7.8) and 0.5 mol L^{-1} sodium phosphate (pH 6.8) were used as eluents. The flow rate was 2 mL min^{-1}. Compounds **4**−**7** were detected by UV absorbance at 270 nm. Nucleoside mono-, di-, and triphosphates and oligodeoxynucleotide were recorded at a wavelength of 260 nm and zoledronate at a wavelength of 218 nm. The concentration of the eluted compounds was 0.3 mmol L^{-1}.

Acknowledgment. The authors thank Evelina Laitinen, M.Sc., and Heidi Isotalo for their skillful help in performing the kinetic measurements and Dr. Sergei Mikhailov and Dr. Nelly Padyukowa (Engelhardt Institute of Molecular Biology, Russian Academy of Sciences, Moscow, Russia) for the preparation of compounds **4** and **5** and Dr. Andrei Guzaev (AM Chemicals, Oceanside, CA, USA) for the preparation of compounds **6** and **7**.

JO800317E

(18) Andreeva, O. I.; Efimtseva, E. V.; Padyukova, N. S.; Kochetkov, S. N.; Mikhailov, S. N.; Dixon, H. B. F.; Karpeisky, M. Y. *Mol. Biol.* **2001**, *35*, 717–729.